The Abdus Salam
International Centre for Theoretical Physics

United Nations
Educational, Scientific
and Cultural Organization

International Atomic
Energy Agency

SMR.1744 - 5

SCHOOL ON ION BEAM ANALYSIS AND ACCELERATOR APPLICATIONS

13 - 24 March 2006

Ion Beam Analysis - Applications in materials science

Gabor BATTISTIG
Research Institute for Technical Physics and Materials Science
Budapest, Hungary

Strada Costiera 11, 34014 Trieste, Italy - Tel. +39 040 2240 111; Fax +39 040 224 163 - sci_info@ictp.it, www.ictp.it

Ion Beam Analytical methods and applications in Materials Science

Gábor Battistig

Research Institute for Technical Physics
and
Materials Science
(MTA - MFA)
Budapest, Hungary

battisti@mfa.kfki.hu

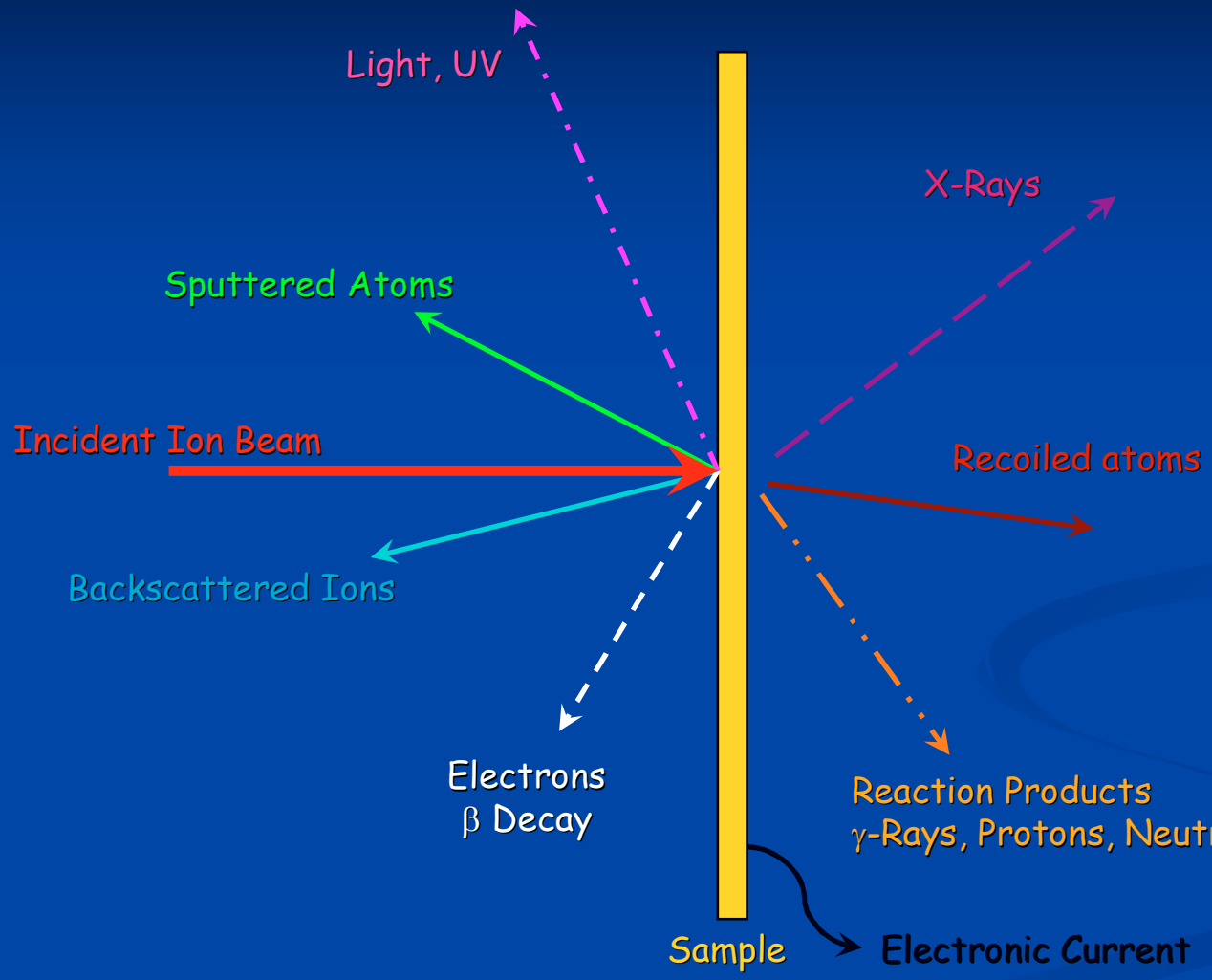

Electrostatic Accelerator
$^1H^+$, D^+, $^3He^+$, $^4He^+$, ……
100 keV – 10 MeV

Rutherford Backscattering Spectroscopy (RBS)

Auger Electron Spectroscopy (AES)

Secondary Ion Mass Spectroscopy (SIMS, SNMS)

Luminescence

Elastic Recoil Detection (ERD)

Particle Induced X-Ray Emission (PIXE)

Nuclear Reaction Analysis (NRA)

Ion Beam Induced Current (IBIC)

Ion beam analytical techniques

Acronym		Interaction
RBS	**R**utherford **B**ackscattering **S**pectrometry	Elastic scattering at backward angles
ERDA or FRS	**E**lastic **R**ecoil **D**etection **A**nalysis, **F**orward **R**ecoil **S**pectroscopy	Elastic recoil at forward angles, not necessarily Rutherford
NRA	**N**uclear **R**eaction **A**nalysis	Nuclear reaction between incident beam and nuclei in the target, producing a light charged particle.
NRP or r-NRA	**N**uclear **R**esonance **P**rofiling, resonant **N**uclear **R**eaction **A**nalysis	Exploitation of narrow nuclear resonances via scanning of the incident beam energy.
PIXE	**P**article-**I**nduced **X**-ray **E**mission	Characteristic X-ray emission following ionization by the primary beam.
PIGE	**P**article-**I**nduced **G**amma **E**mission	Prompt gamma emission during ion beam irradiation

Main questions relevant to the study of the near surface regions of materials

- Atomic composition / concentration profiles
- Atomic structure, crystallinity
- Atomic movements (transport)

Most used analytical techniques

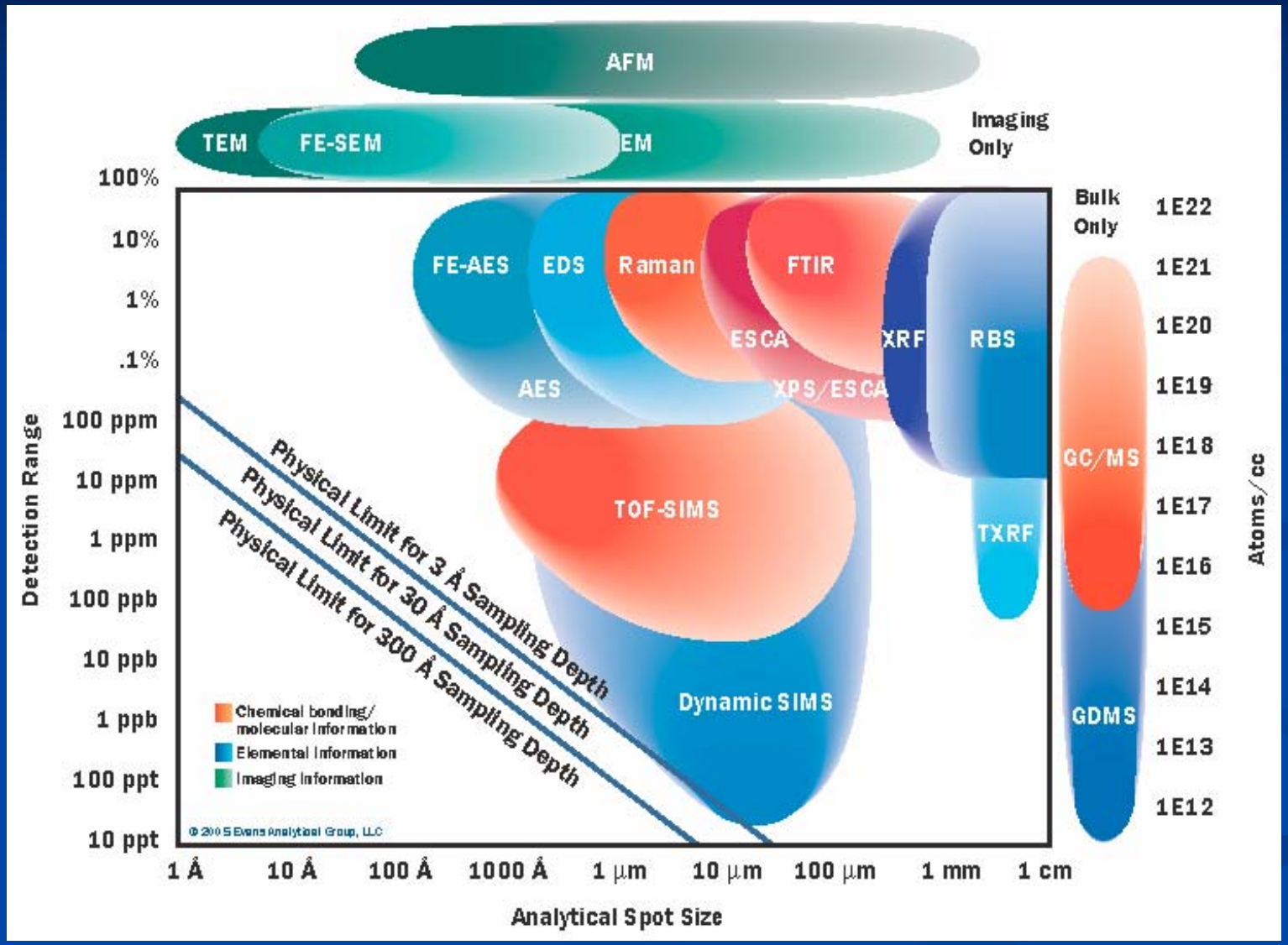

SIMS, SNMS

An energetic ion beam is used to sputter atoms from the surface. Secondary ions emitted are mass analyzed.
Sensitivity ≈ 10^{12} – 10^{14} atoms/cm^3
Depth resolution ≈ 10 – 200 Å
Lateral resolution ≥ 1 μm (imaging)

TXRF

X-rays incident at very shallow angles excite the surface atoms. The atoms relax through the emission of a characteristic X-ray.

Depth resolution ≈ 30 – 80 Å

FTIR

Infrared beam excites the sample, molecular constituents vibrate in the IR regime. The molecules, surrounding environments and concentrations of the oscillating chemical bonds may be determined.

Depth resolution ≈ 0.1 – 1 μm

Raman

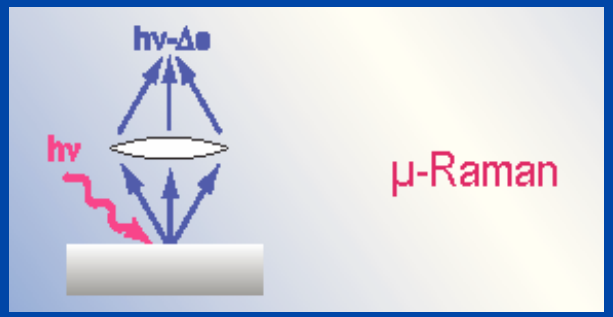

It measures the intensity of light scattered inelastically off the sample as a function of the wavelength. Chemical bonds gain or lose characteristic amount of energy, that correspond to different vibrational modes in the bonds.

XPS

Surface of the sample is excited with X-rays, photoelectrons are emitted from the atoms near the surface. Chemical bonding information may be determined.

Depth resolution ≈ 10 – 100 Å
Detection limit ≈ 0.001 – 1 at%

AES

Focused electron beam produces Auges electrons with discrete energies, specific to each element. (Escape depth ≈ 10 Å) (Sputtering is needed.)
Depth resolution ≈ 20 – 200 Å
Detection limit ≈ 0.1 – 1 at%

SEM / TEM

Finely focused e-beam is rastered over the sample surface, its image is formed from secondary electros and photon emission. Energy dispersive X-ray (EDX) spectroscopy is also possible – elemental quantification.

STM / AFM

A very sharp tip, located a few Å of the surface, is rastered over the sample surface. Surface morphology and physical properties are measured.

SE

Polarized light scattered on the sample surface, complex refractive index can be determined, layer structure can be obtained. Good depth scale!

Methods:

- Ion beam techniques (IBA): RBS, MEIS, ERD, NRA, resonance depth profiling, PIGE, PIXE, channeling, AMS …
  "Non-destructive", in situ, at atmospheric pressure

- Sputtering techniques: SIMS, SNMS, AES …..
  Destructive

- Microscopy: SEM, TEM, Electron probe …..
  "Non-destructive or destructive", sample preparation artefacts

- X-ray diffraction, XRF …..
  Non-destructive

BUT with these methods: No chemical, electrical, magnetic, optical, mechanical, etc. information.

Complementarity:

IBA ⇔ SIMS ⇔ SEM

- Near field microscopy, STM, AFM .....
- Spectroscopic Ellipsometry

Analytical techniques used to study typical CMOS structure

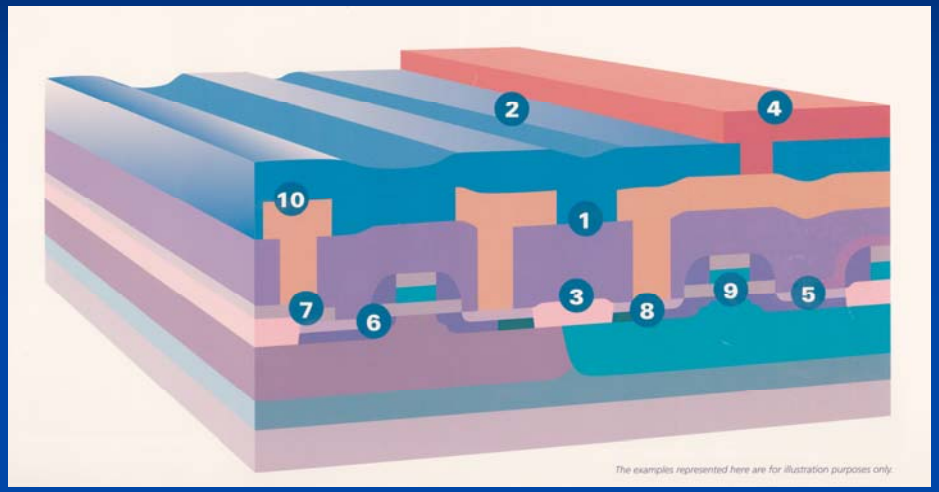

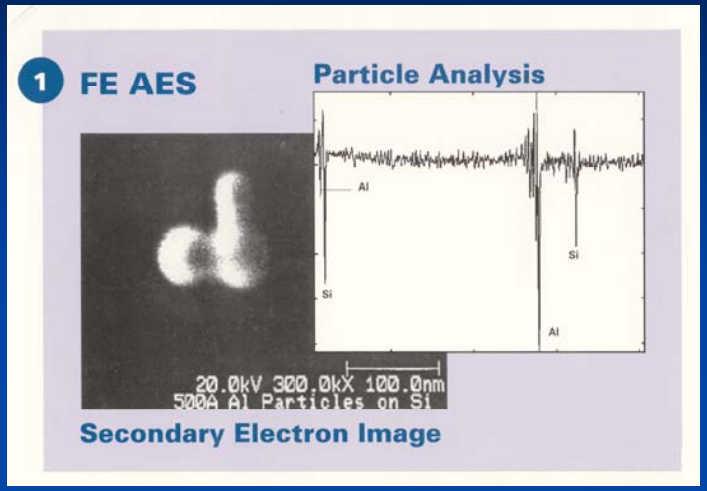

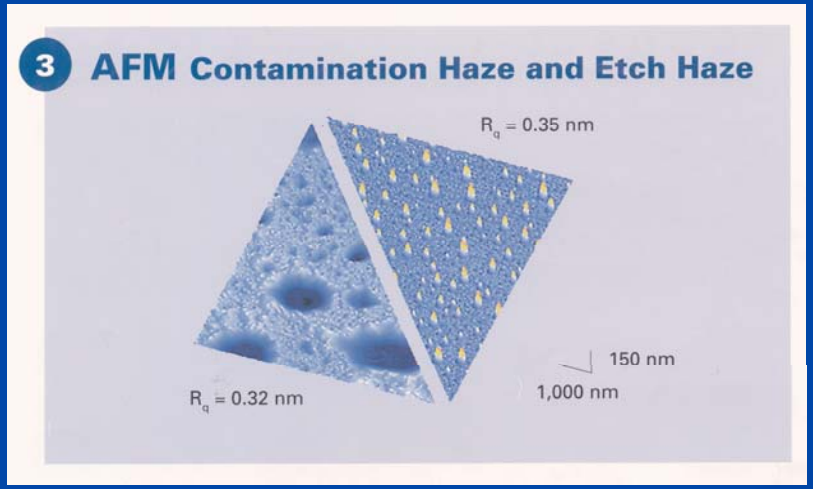

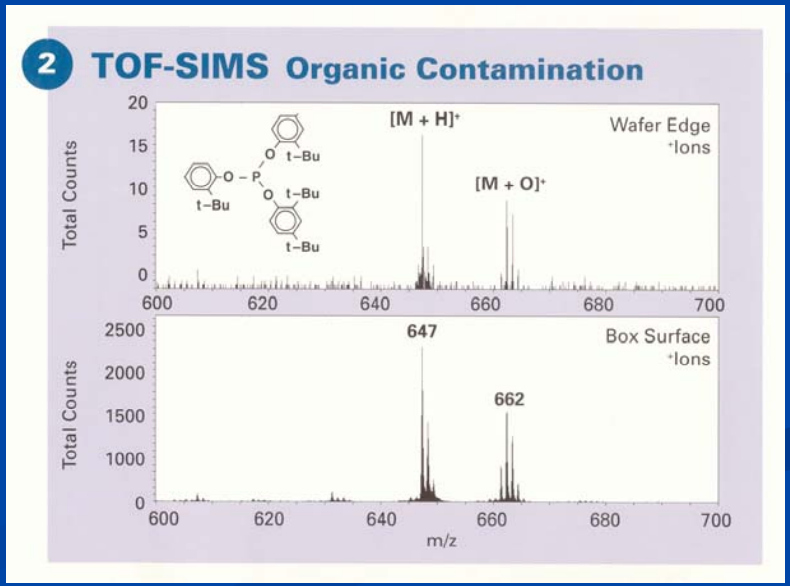

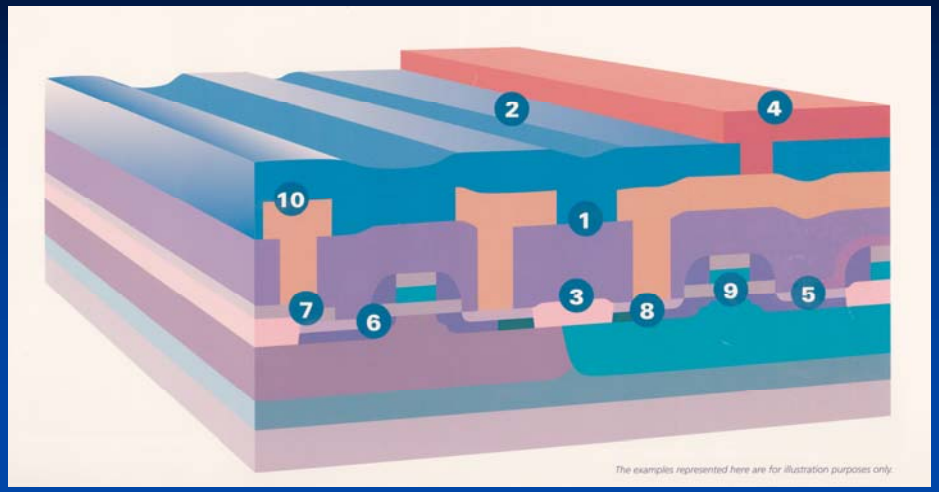
2
4
10
1
7
6
3
8
9
5
The examples represented here are for illustration purposes only.

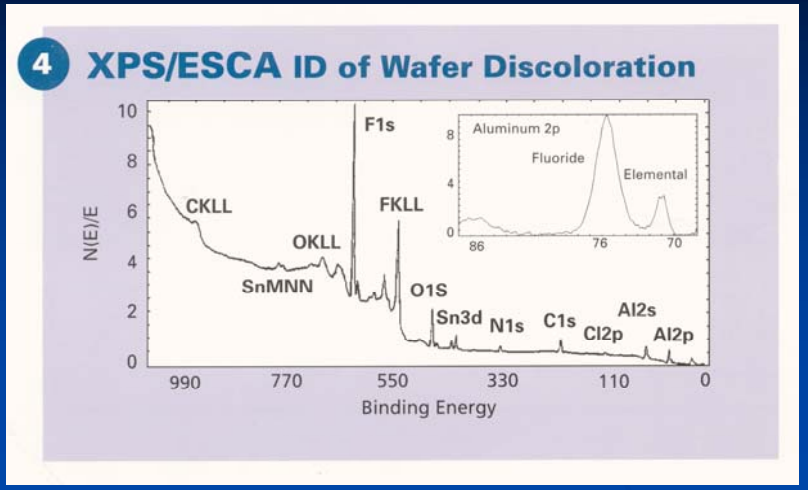
4 XPS/ESCA ID of Wafer Discoloration
N(E)/E
CKLL
OKLL
SnMNN
F1s
FKLL
O1S
Sn3d
N1s
C1s
Cl2p
Al2s
Al2p
Aluminum 2p
Fluoride
Elemental
Binding Energy

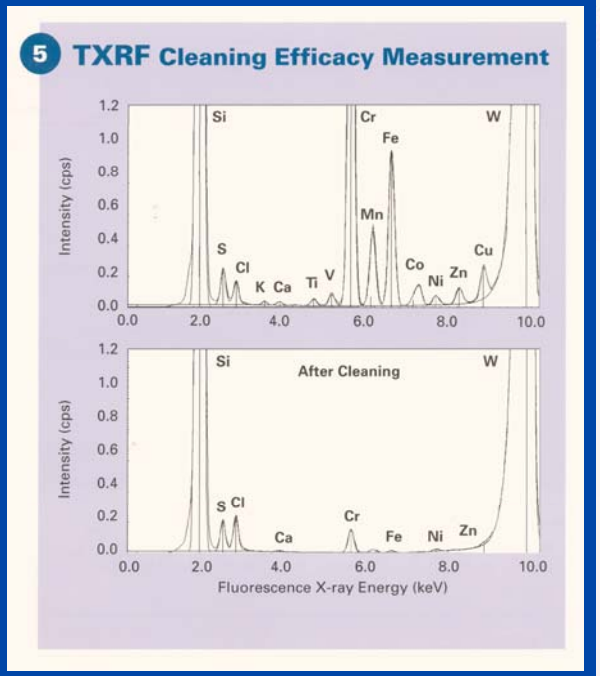
5 TXRF Cleaning Efficacy Measurement
Intensity (cps)
Si
S
Cl
K Ca
Ti
V
Cr
Mn
Fe
Co
Ni
Zn
Cu
W
After Cleaning
Fluorescence X-ray Energy (keV)

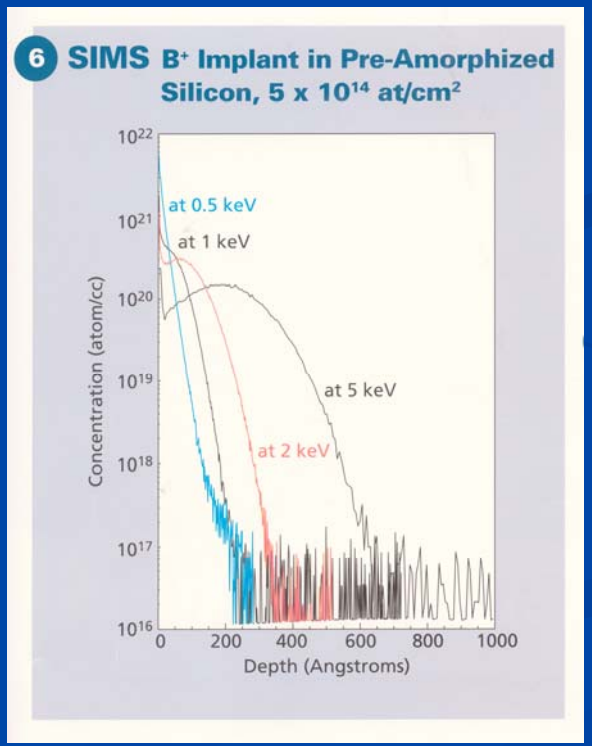
6 SIMS B+ Implant in Pre-Amorphized Silicon, 5 x 10¹⁴ at/cm²
Concentration (atom/cc)
at 0.5 keV
at 1 keV
at 5 keV
at 2 keV
Depth (Angstroms)

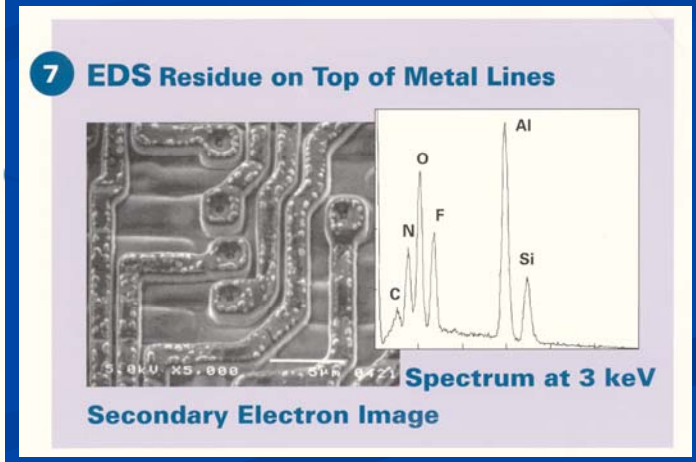
7 EDS Residue on Top of Metal Lines
Al
O
N
F
Si
C
Spectrum at 3 keV
Secondary Electron Image

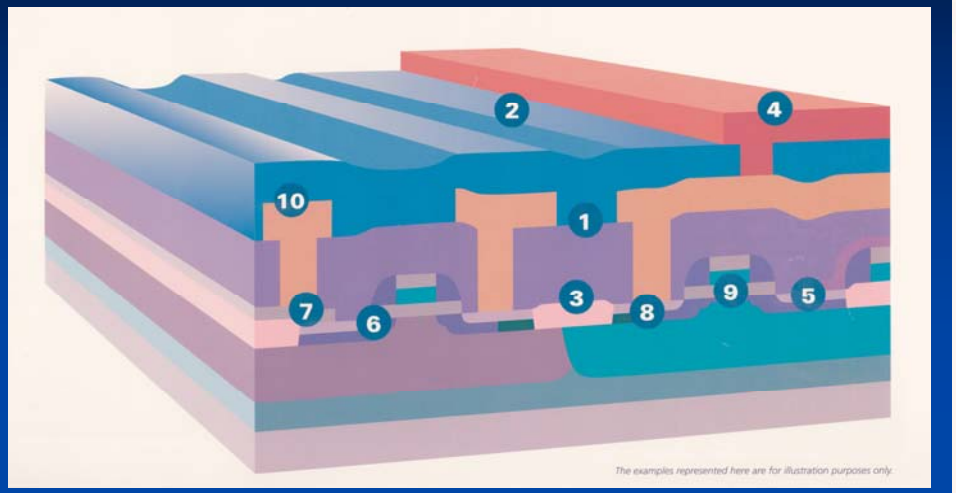
2
4
10
1
7
6
3
8
9
5
The examples represented here are for illustration purposes only.

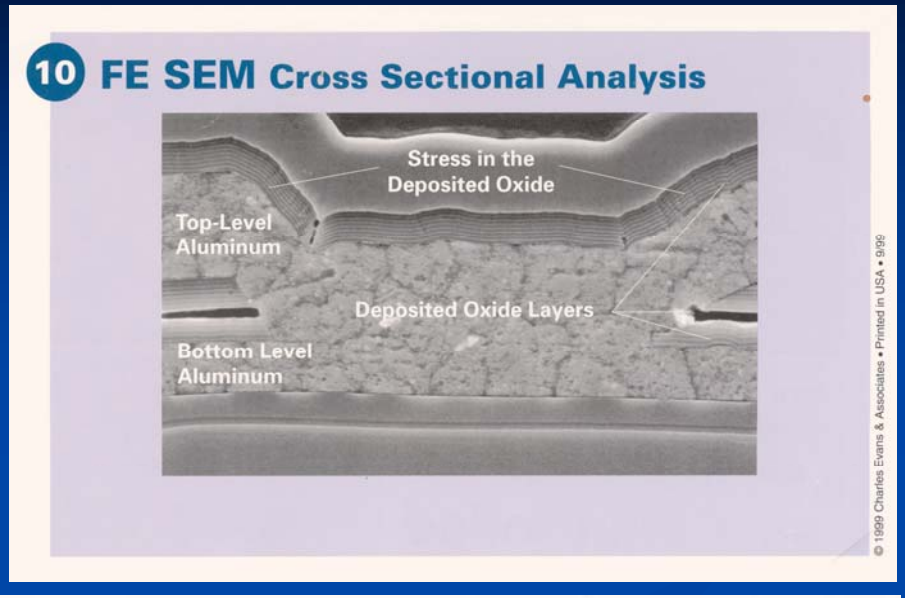
10 FE SEM Cross Sectional Analysis
Stress in the Deposited Oxide
Top-Level Aluminum
Deposited Oxide Layers
Bottom Level Aluminum
© 1999 Charles Evans & Associates • Printed in USA • 9/99

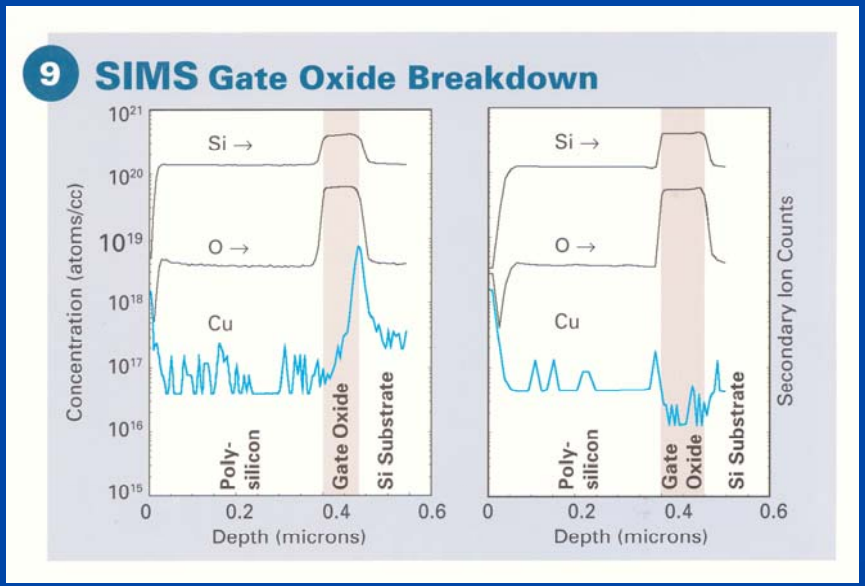
9 SIMS Gate Oxide Breakdown
Concentration (atoms/cc)
Si →
O →
Cu
Poly-silicon
Gate Oxide
Si Substrate
Depth (microns)
Secondary Ion Counts

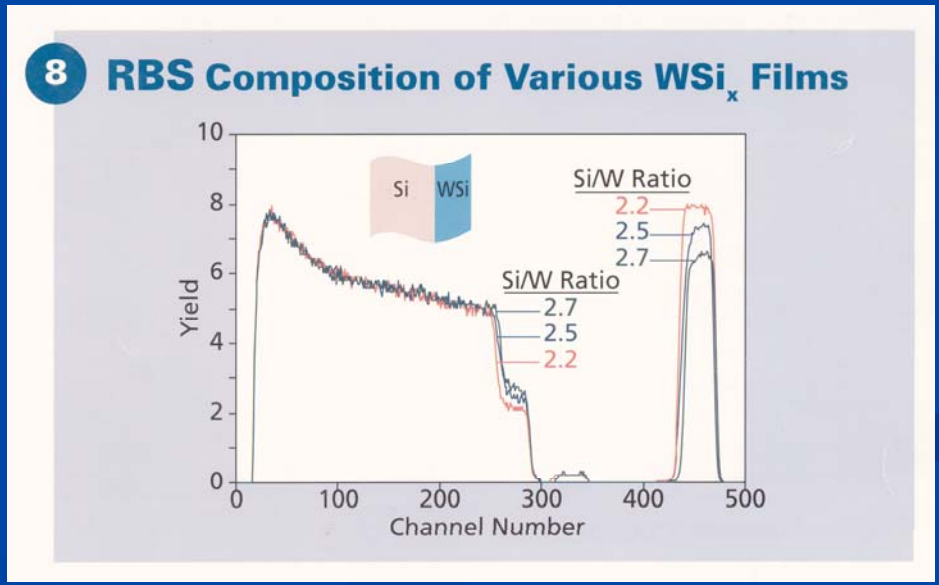
8 RBS Composition of Various WSi$_x$ Films
Yield
Channel Number
Si
WSi
Si/W Ratio
2.2
2.5
2.7
Si/W Ratio
2.7
2.5
2.2

Atomic composition

- **IBA:**

  Matrix independent

  - Absolute areal density in thin films – at/cm^2 (↘ 10^{11} — 10^{12})
  - Concentration profiles – at/cm^3 (↘ 1-100 ppm)
  - Depth scale well defined (10Å — 10μm)
  - μBeam (lateral resolution ↘ ~1μm but possible beam damage)
  - NRA: isotope specific

- **SIMS, AES:**

  Matrix dependent yield, over ~50Å integrated yield

  - Excellent sensitivity and mass discrimination, but preferential sputtering, crater formation, ...faceting effects, possible giant roughening
  - Depth scale given through sputtering rate, only reliable in special cases, calibration is required
  - high resolution mapping

Atomic composition

- **Microscopy:**
  Only structural information, atomic resolution
  - with electron probe (X-ray detection): composition, but high Bremstrahlung, background, integration over ~1 μm^3

Atomic Structure

- **IBA:**
  Channeling
  – information in direct space, crystal structure, defects, lattice location; amorphisation and recrystallisation studies....

- **SIMS, AES:**
  - No structural information

- **Microscopy:**
  – atomic resolution, defect identification (e-diffraction), but no elemental information

- **X-ray diffraction:**
  - lattice identification, phases

Atomic movements

Main questions:
diffusion, implantation, annealing, solid state reactions, growth mechanisms .....

- **IBA:**
  Isotopic tracing with rare isotopes
  - Resonant NRA, RBS, MEIS .....

- **SIMS, AES:**
  - Good mass separation, high sensitivity, but strong sputtering effects

- **Microscopy:**
  - No, but defect identification and evolution

- **X-ray diffraction:**
  - Lattice identification, phases

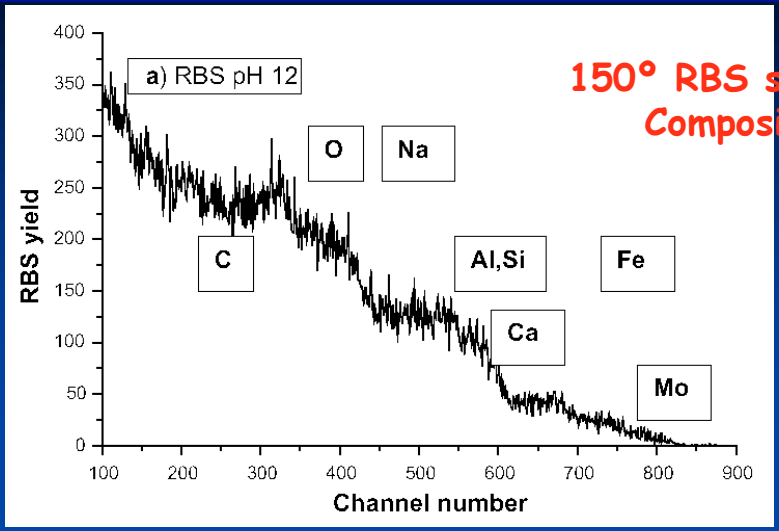

150° RBS spectrum
Composition

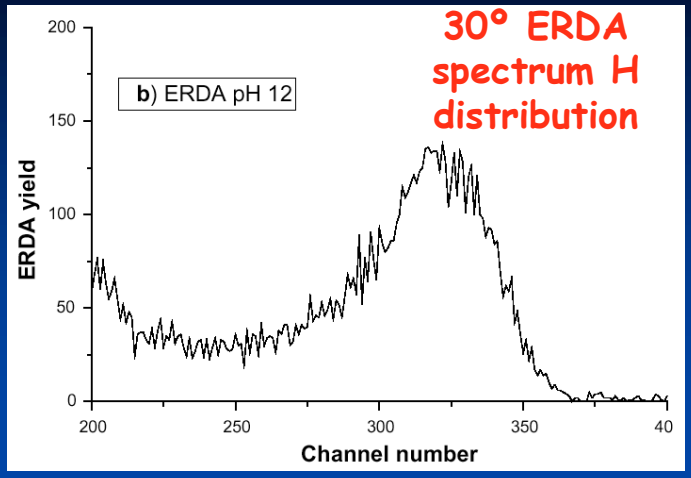

30° ERDA
spectrum H
distribution

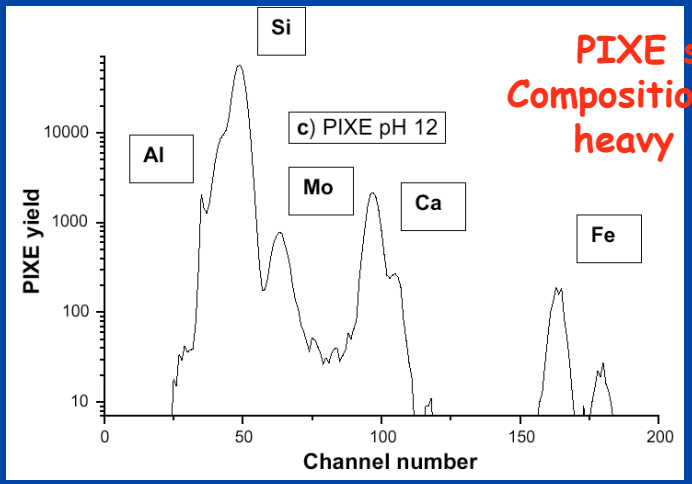

PIXE spectrum
Composition of medium
heavy elements

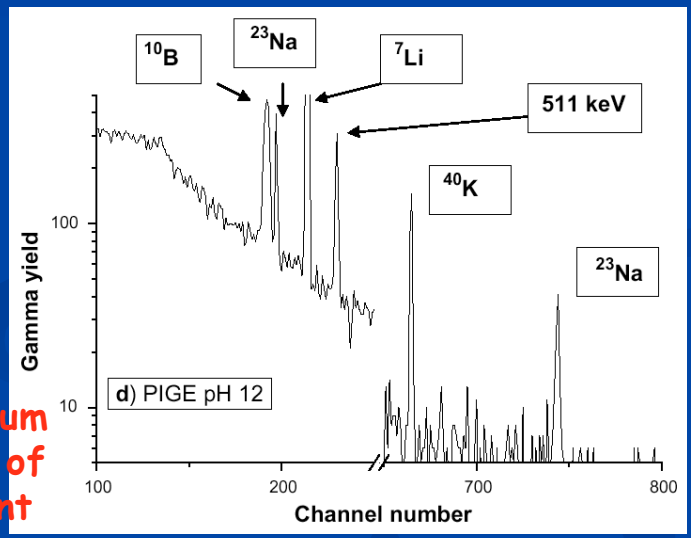

PIGE spectrum
Composition of
light element

Alkali borosilicate glass samples after leaching at 90°C, 7 days at pH=12. Glass dissolution rate is high at pH 0 and 7, while it is strongly reduced at 12, due to the presence of Fe and Mo containing phases near the surface. Homogeneous hydration of the glass surface.

J.Chêne and P. Trocellier Journal of Non Crystalline Solids 337 (2004) 86-96, Fig. 5

Structural information Channeling

Experimental angular scans for Nb-BS, Nb-PIXE, Co-PIXE in 0.2 mol% Co doped $LiNbO_3$ for the five major axes. Simulations using the CASSIS program for Nb-BS, Nb-PIXE and Co-PIXE (the latter with the assumptions that Co occupies exclusively Li sites or exclusively Nb sites) are also shown.

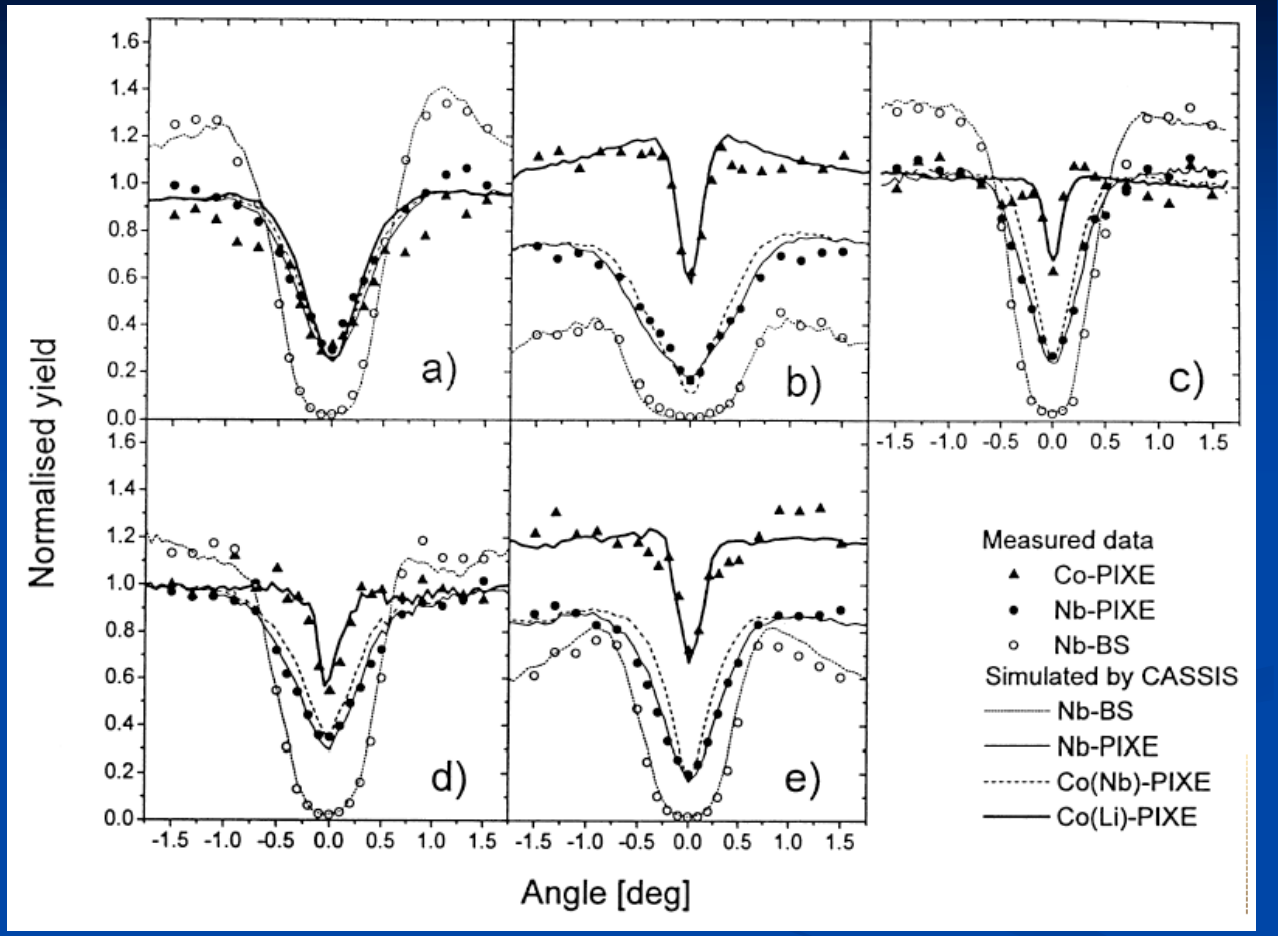

The normalised yields were determined for: (a) ‹0001› at 50° with respect to the (01-10) plane; (b) ‹02-21›. within the (1-102) plane; (c) ‹01-10› at 15° with respect to the (2-1-10) plane; (d) ‹0-441› at 80° with respect to the (2-1-10) plane; and (e) ‹11-20› within the (0001) plane.
The channneling measurements proved that the lattice site of Co in low-doped congruent $LiNbO_3$ is a regular Li-site, a crucial finding for interpreting ^{57}Co Mössbauer effect experiments.

E. Szilágyi et al. Solid State Com. 115 (2000) 535 Fig.3

Micro-RBS mapping of particulates from laser deposited $Si_{1-x}Ge_x$ thin films on Si

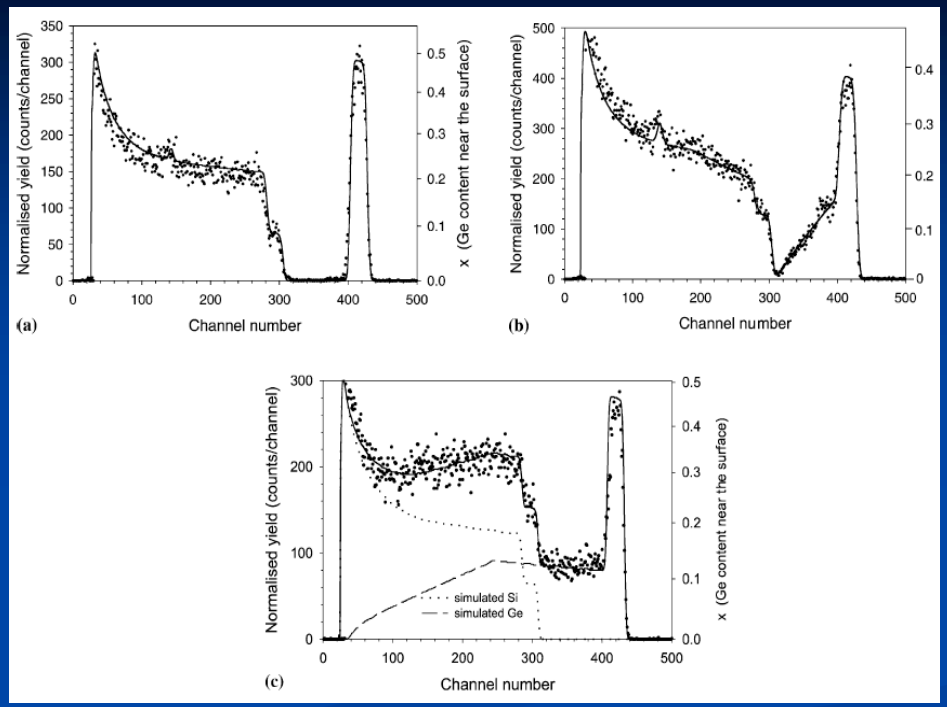

(a) Ge elemental map

(energy window between ch.320 and 390, 65 × 65 mm2 scanning area, 128 × 128 pixel),

(b) tomographic image created from 15 pixels wide region between the vertical lines.

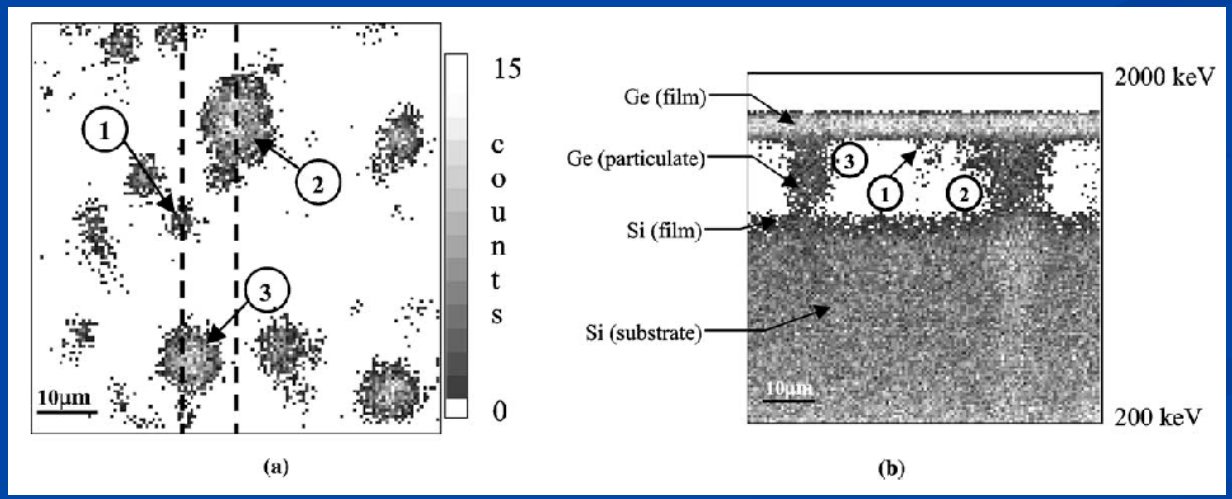

A.Simon and Z.Kántor, NIMB 190 (2002) 351 –356, Figs. 3 and 4

High depth resolution isotopic tracing by ^{18}O with MEIS (100 keV protons)

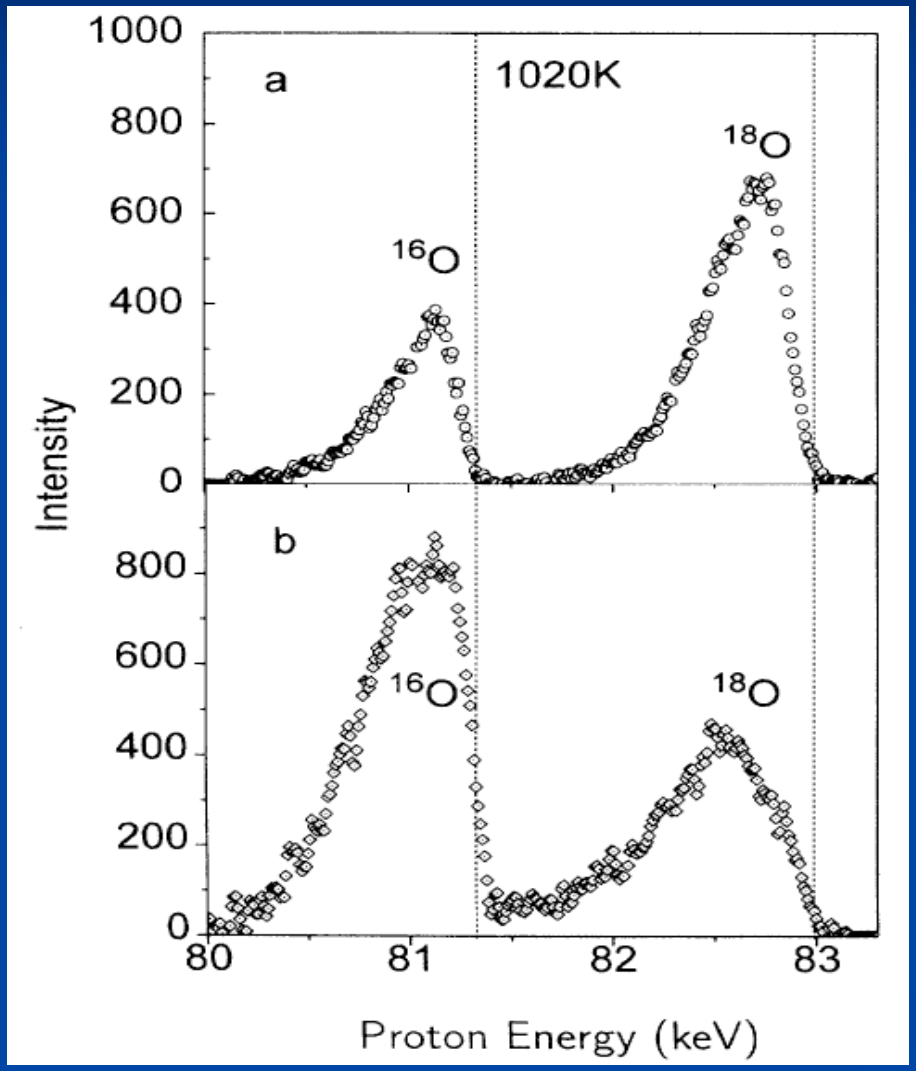

Study of growth mechanisms of ultrathin oxide films on Si, here in the 15-25Å range. Overlapping isotope depth profiles are found, in contrast to thicker films (>40 Å). After 165 mn exposure the growth rate is strongly reduced and ^{18}O loss is observed. Combination of MEIS with LEIS, XPS and spectroscopic ellipsometry led to a detailed picture of the mechanisms of the first stages of thermal growth of oxide on Si.

MEIS spectra for Si(100) samples oxidized at 1020 K and 10^{-2} Torr. Exposure in $^{18}O_2$ were 10 min for both samples. This first oxidation step is followed by oxidation in $^{16}O_2$ for (a) 165 min and (b) 2640 min.

E.P. Gusev et al. Phys. Rev. B52 (1995) 1759. Fig.6

^{30}Si isotopic tracing study of Si self diffusion in olivine of geophysical interest

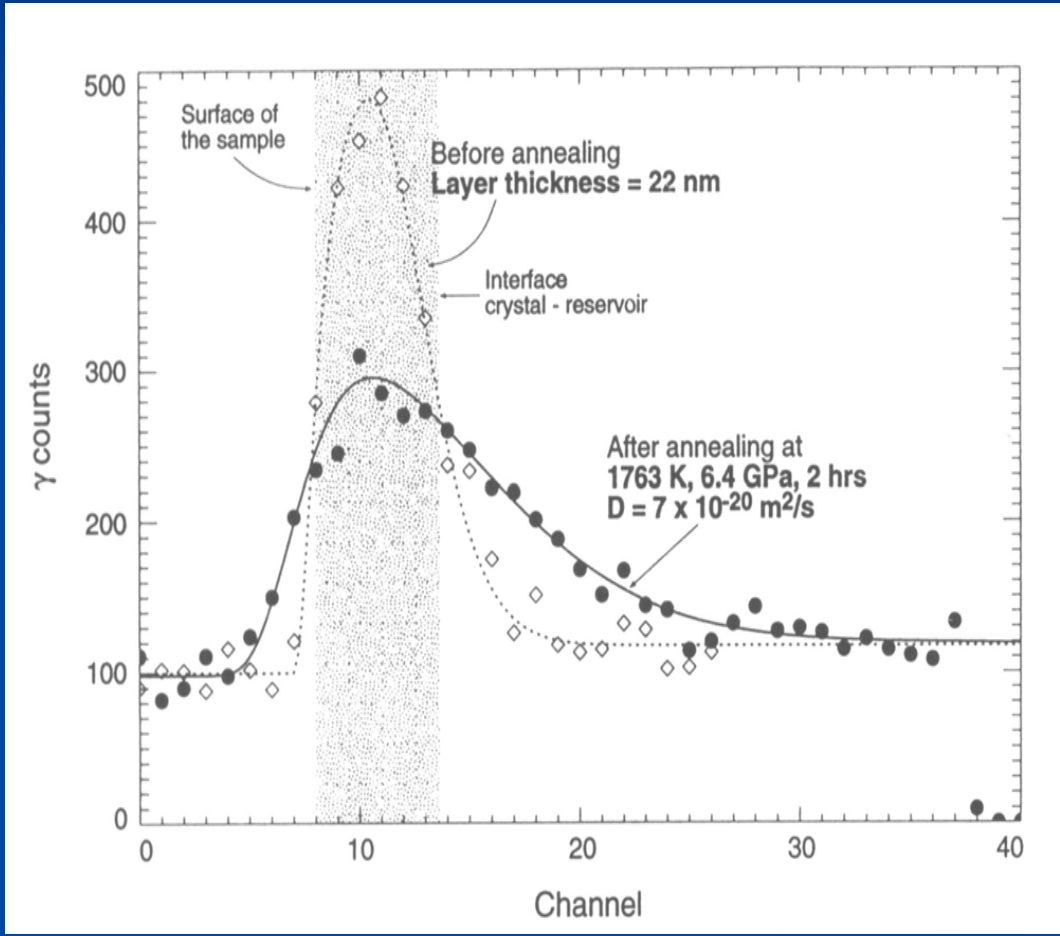

A ^{30}Si enriched 22 nm thick fosterite layer was deposited by sputtering on the sample and annealed at 1763 K and 9 GPa. The high resolution resonance depth profiling of ^{30}Si (^{30}Si(p,γ)) at 620.4 keV, Γ=70 eV) yields the self-diffusion coefficient of Si. From that the viscosity in extreme conditions of olivine, very abundant in the earth mantel, may be calculated.

Fosterit: Mg_2SiO_4
Olivine: $(Mg,Fe)_2SiO_4$

F. Bejina et al. Geophysical Research Letters 24 (1997) 2597, Fig.2

Multilayer structures

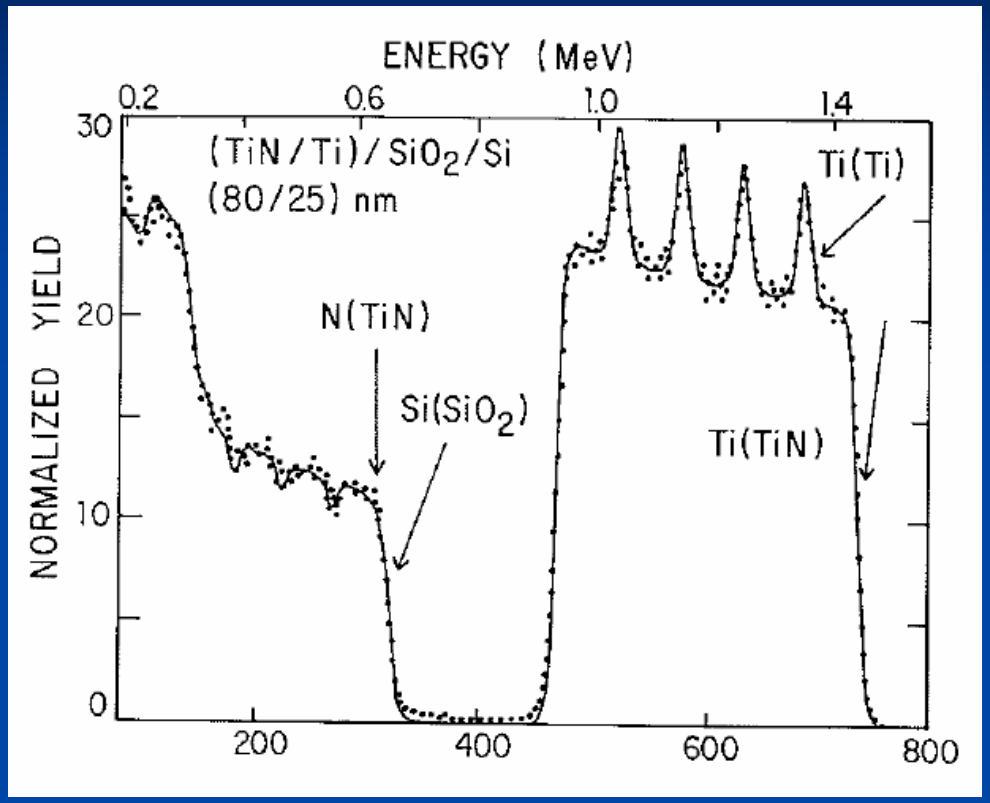

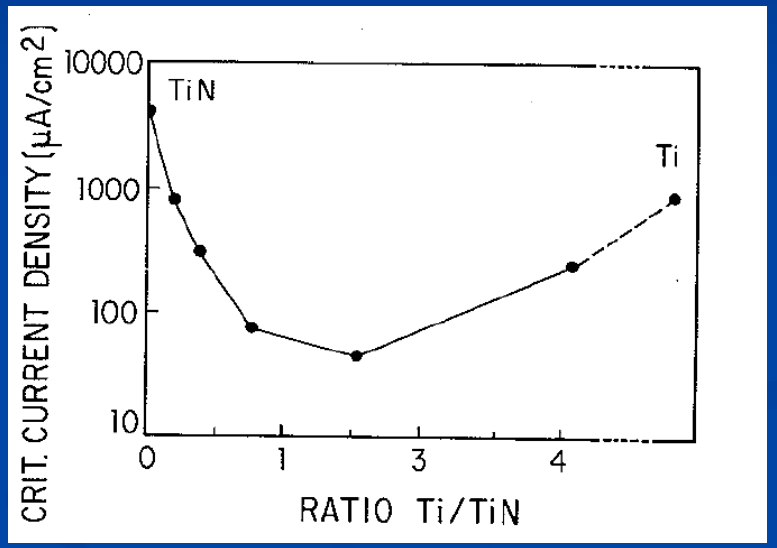

Reactive magnetron deposited multilayered TiN/Ti thin film coating is adherent, stress free, fully dense. 0.5μm coatings produce same performance as 3μm single layered ones. Precise knowledge of the compositions and thickness ratios is essential for optimising hardness, elasticity and aqueous corrosion protection. a) 2 MeV α-RBS spectrum showing the individual layers. b) critical current density vs TiN/Ti ratio for iron dissolution in cyclovoltametric aqueous corrosion tests of coated carbon steels, determined by RBS. ^{14}N was also measured with $^{14}N(d,\alpha)$ reaction.

I.J.R. Baumvol, NIMB, 85 (1994) 230, Fig.3

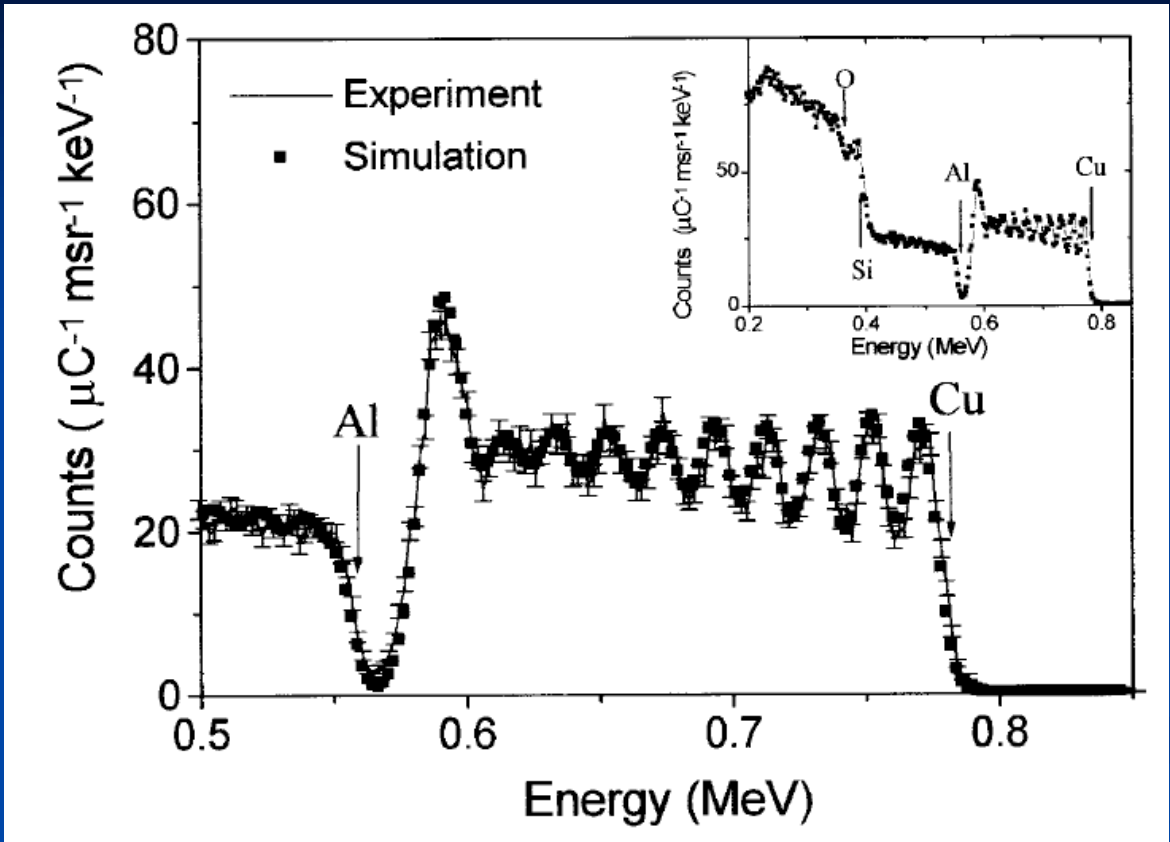

The formation of Cu:Al_2O_3 composite films on Si(001) with alternate pulsed laser deposition yielding nucleated Cu nanocrystals with tailored configuration embedded in Al_2O_3 was studied in view of their special optical, electrical and magnetic properties. The Cu content of up to 10 successive layers was measured individually with 1 MeV α-RBS and 42° tilted sample. The first Cu deposit directly on the Si substrate is ~ twice as rich as the others. In combination with high resolution TEM full information on the growth process was obtained.

R. Serna et al. Appl. Phys. A 71 (2000) 583. Fig. 1

This powerful technique may be extended to many fields of Materials Science not related to Museum research

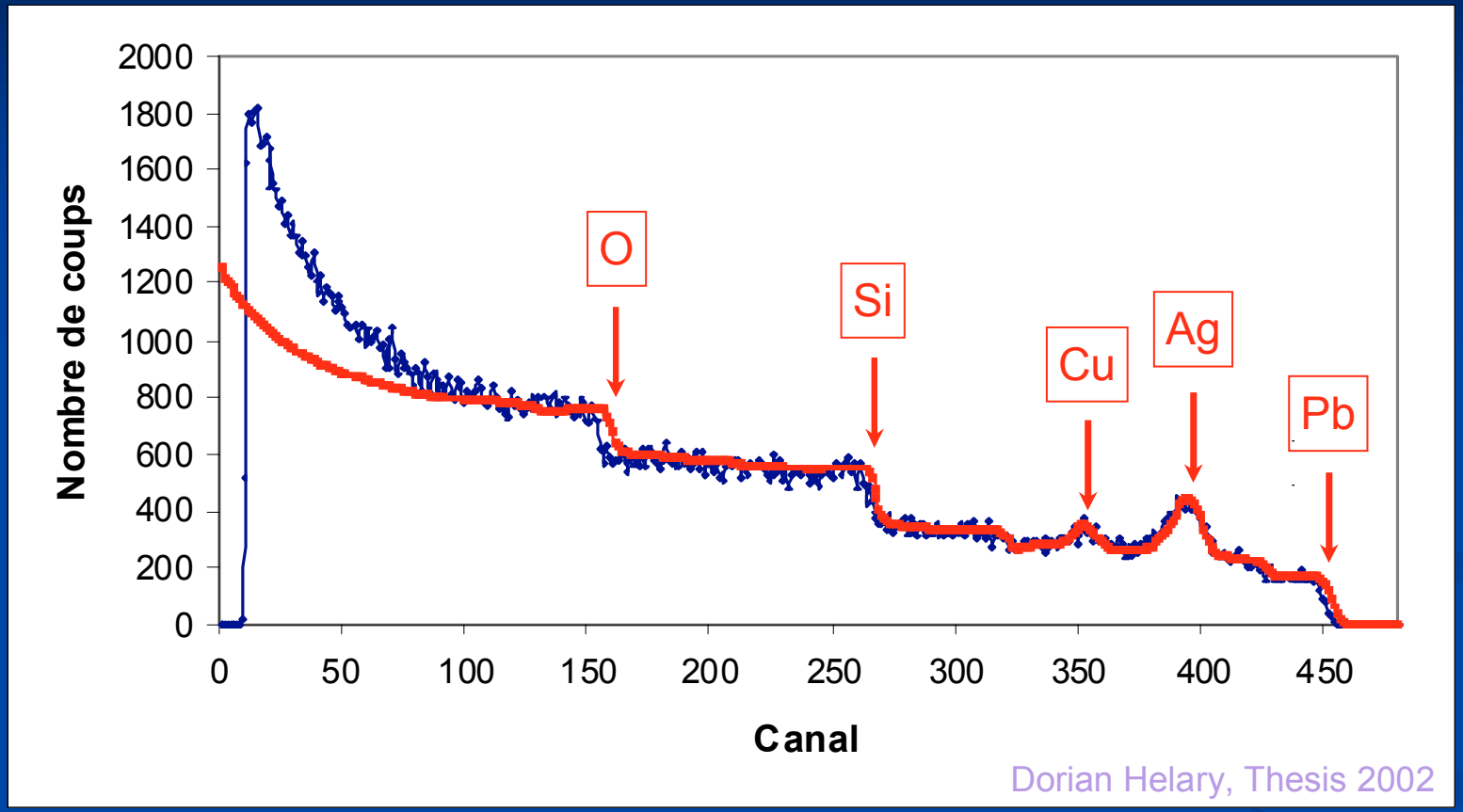

Dorian Helary, Thesis 2002

Experimental (blue) and SIMNRA simulated (red) 3 MeV α-RBS spectra obtained from a lustered islamic ceramics. Beam diameter 50mm, extracted in He.
Majors (averaged over 6 layers): Pb 0.6%, Ag 3%, Cu 3%, Ca 3%, Si 30%, O 60%.
Overall thickness of the luster 760nm.
The first layer (40nm) contains no heavy metal and is transparent, a new finding.
Measurements with beams extracted in He - Louvre Laboratory, J. Salomon et al.

Tsuba patinas

RBS spectra NRA spectra

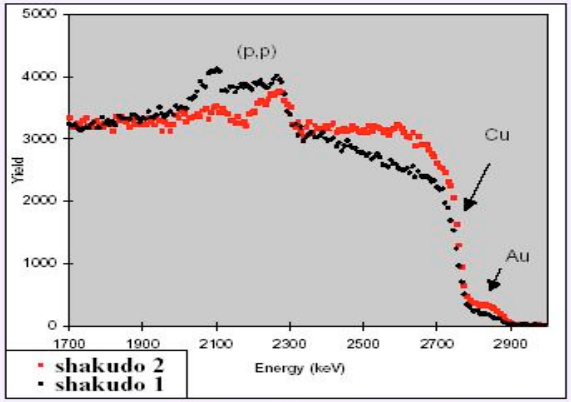

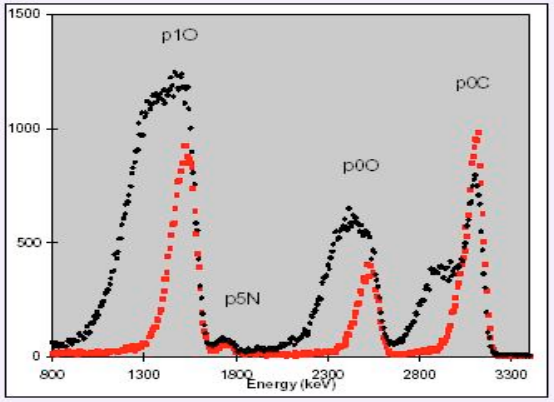

Traditional Japanese shakudo

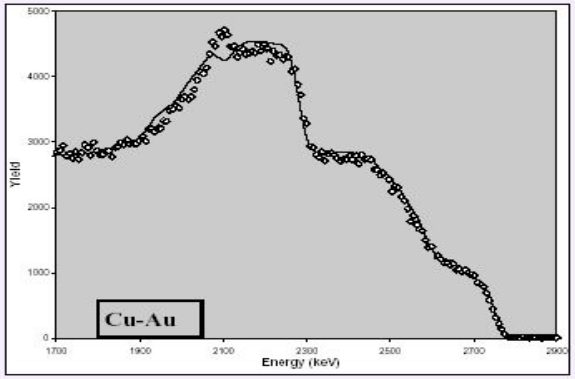

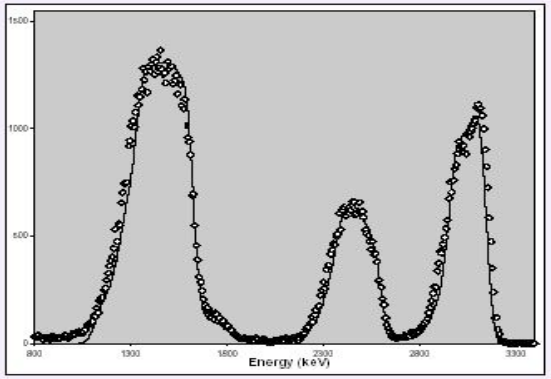

Experiment
RBS protons at 3 MeV
NRA deuterons at 2.3 MeV
(d,p) reactions, C, N, O

Results
The combination of the three techniques allows us to identify the composition and tells us the thickness of the patina layer. This is a precious gide for understanding the fabrication techniques.
The figure shows modern and traditional patinas. Once the fabrication technique is known it can be used as an artist signature for identification (fingerprint).

Tsubas are Japanese sword gards. Shakudo is a Cu-Au alloy (here ~ 4%). The colour of its patina depends on its oxidation state. Red and black dots belong to two different items. with patina thicknesses 1m and ~ 3m. The black spectrum shows some bulk carbon.
Louvre Laboratory, Evanthia Ionnidon Thesis 1999

^{18}O study of oxygen transport mechanisms during plasma oxidation of Si through an ionic conductor

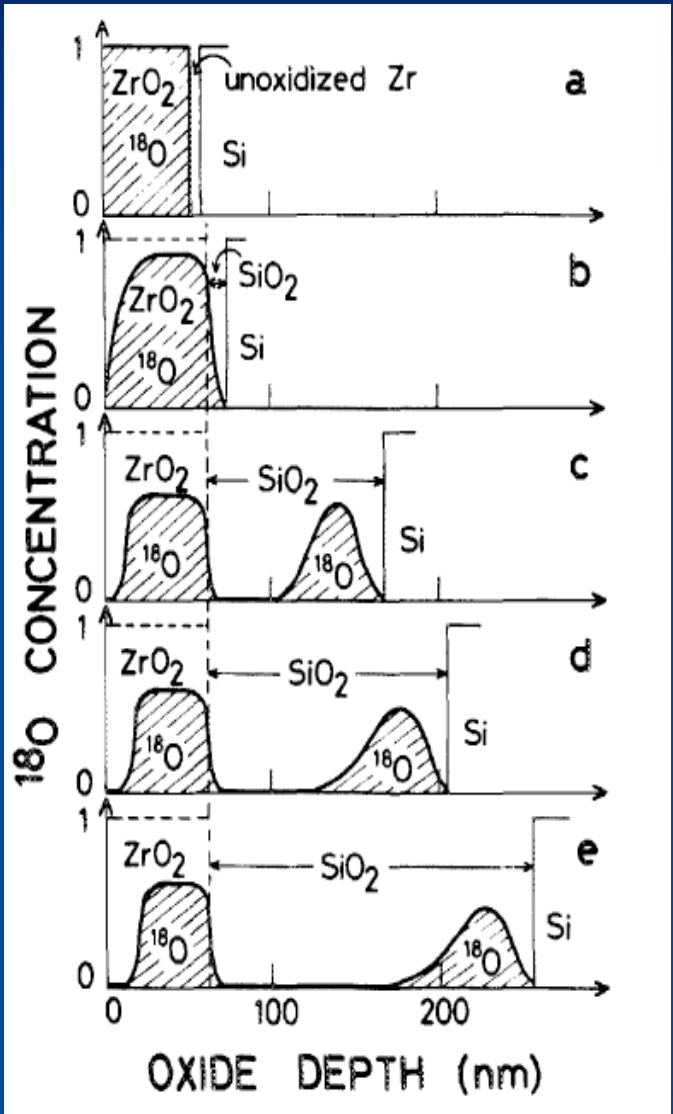

Si does not plasma oxidise directly, but does so through a thin ZrO_2 layer (~60 nm, 84% ^{18}O enriched) formed on its surface, active oxygen being provided by this ionic conductor. ^{18}O tracing with the 629 keV, Γ=2.1 keV resonance of $^{18}O(p,\alpha)$ showed that the oxygen from the ZrO_2 penetrates into the silica layer formed, remaining at the oxide/Si interface via a short range migration process, in contrast with thermal oxidation. The process is nearly temperature independent between 25°C and 600°C.

Siejka et al. J.Appl.Phys 56 (1984) 2720 Figs. 8 and 9

Ion implantation of 6H-SiC

Only possible technique to locally dope SiC. Radiation damage and annealing behavior was followed by RBS+channeling, Spectroscopic Ellipsometry and high resolution XTEM.

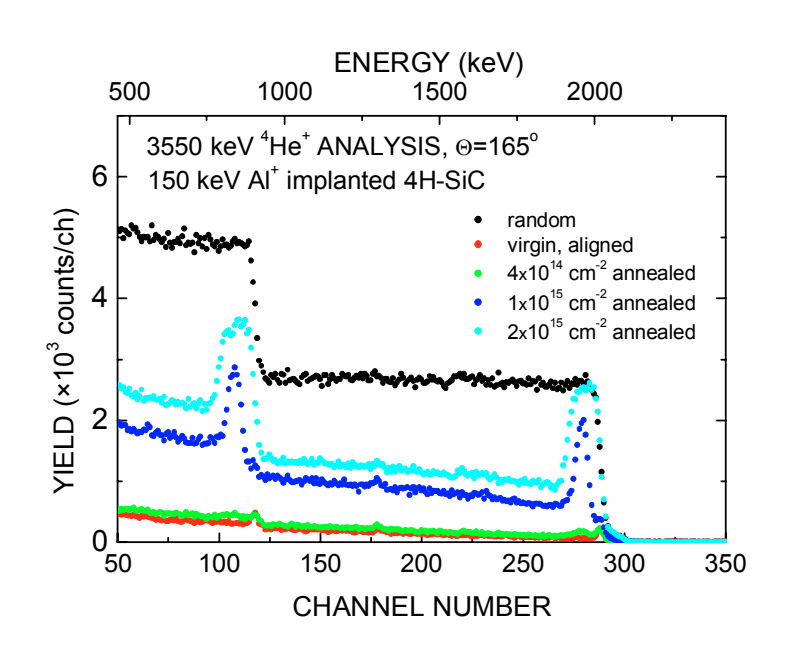

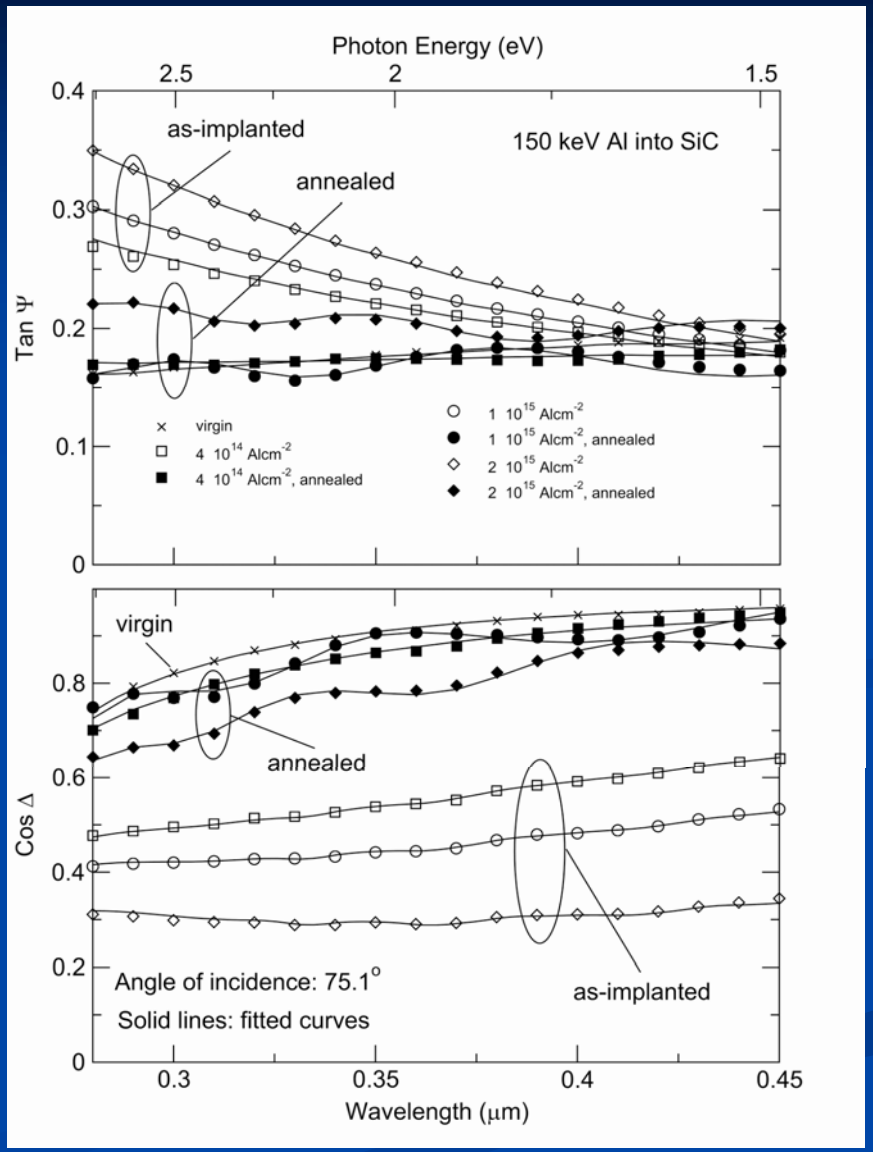

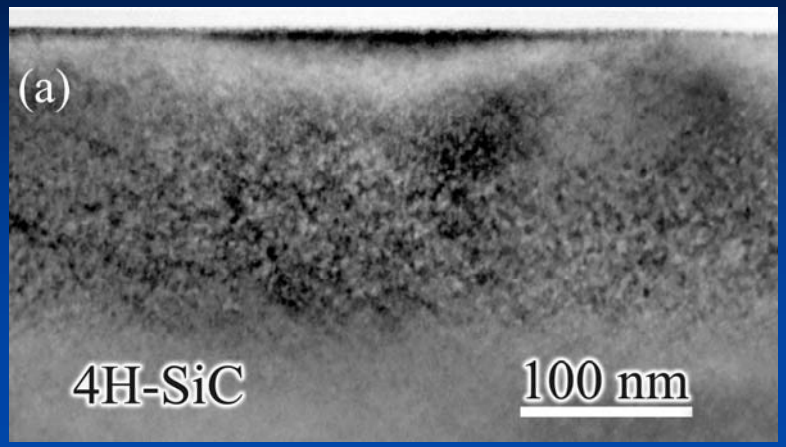

As implanted

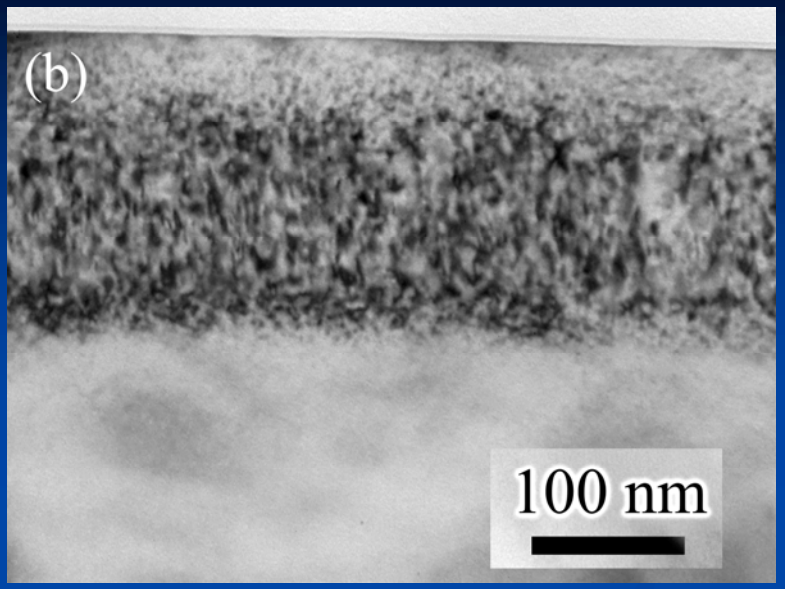

Medium dose, annealed

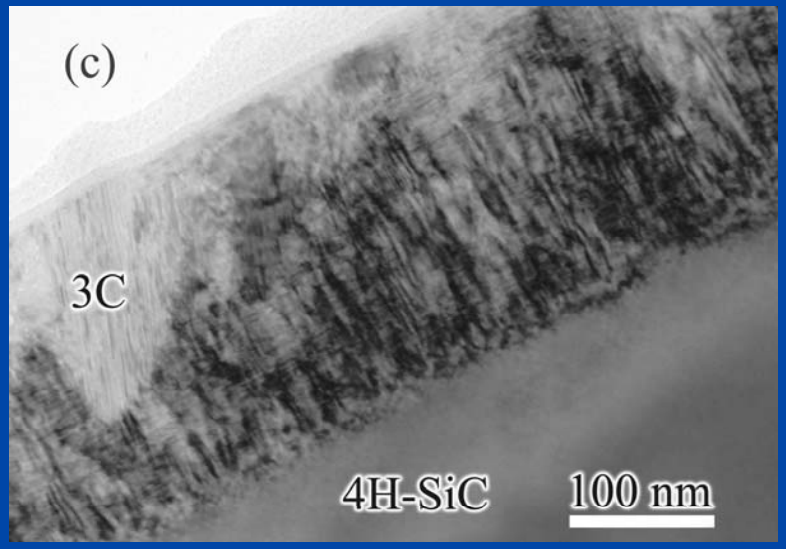

High dose, annealed

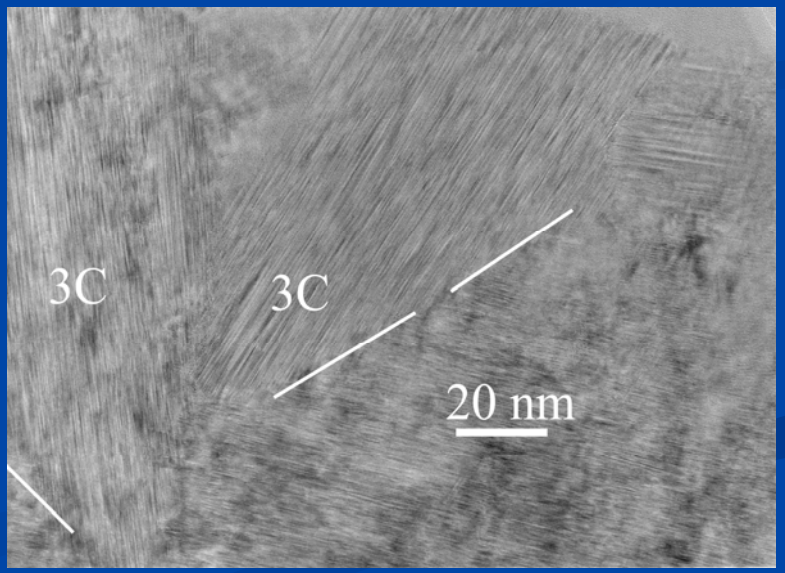

High dose, annealed

Ion implantation of 6H-SiC

Resonance in the $^{12}C(\alpha,\alpha)^{12}C$ cross section at 4.26 MeV. By varying the beam energy the C concentration can be mapped in a simple RBS experiment.

Study of ion implantation induced damage in 6H SiC crystal.

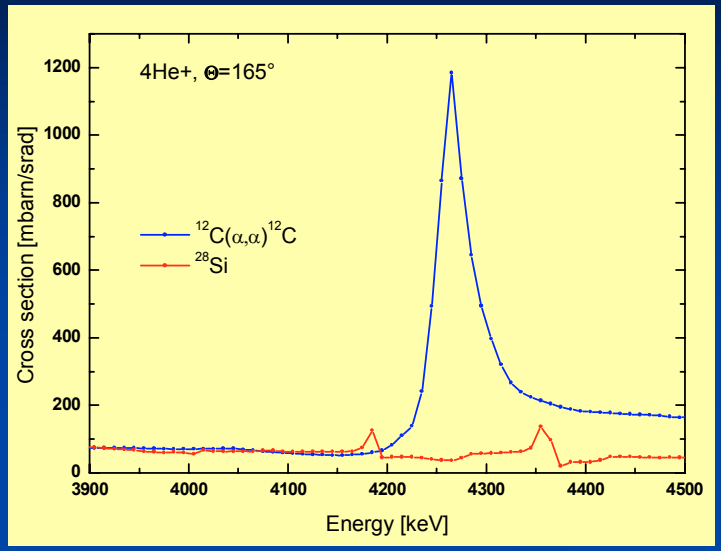

Random direction

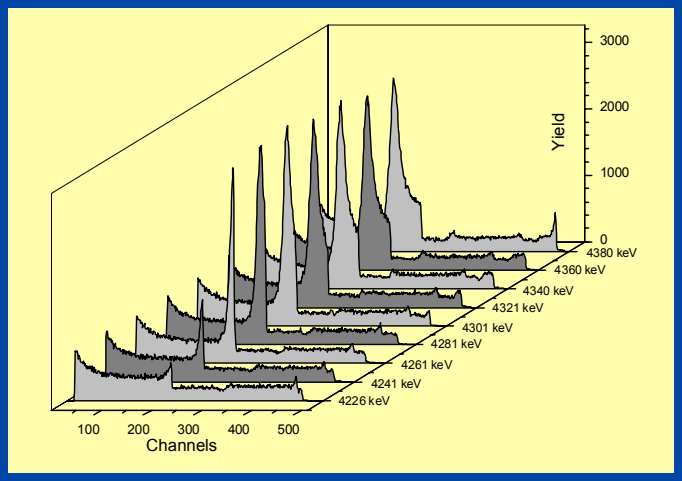

Aligned with C axis

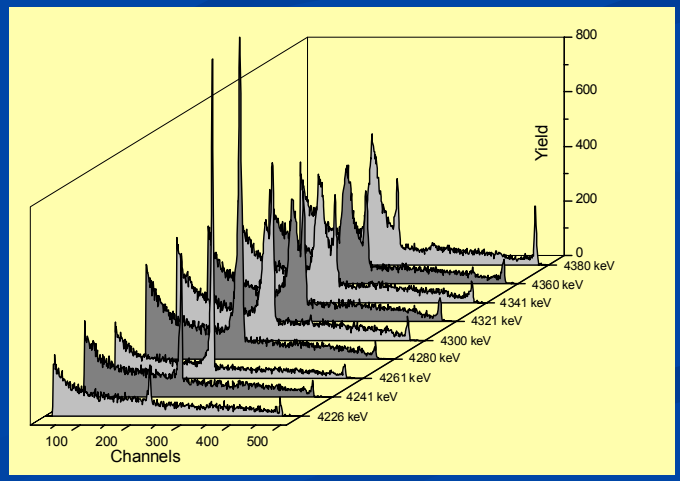

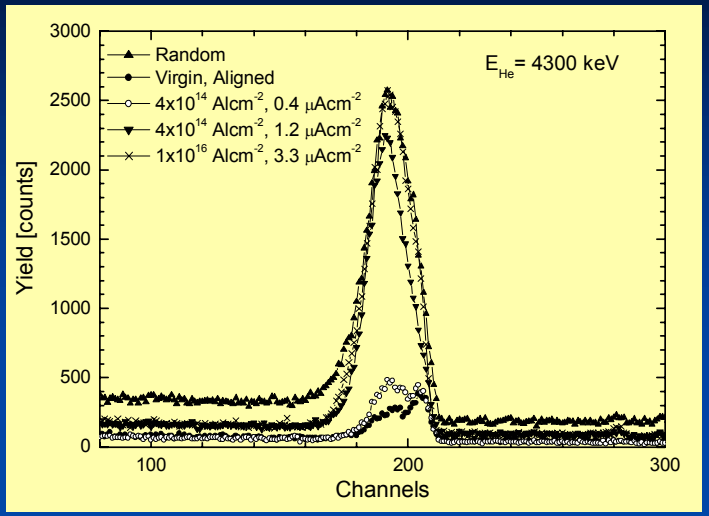

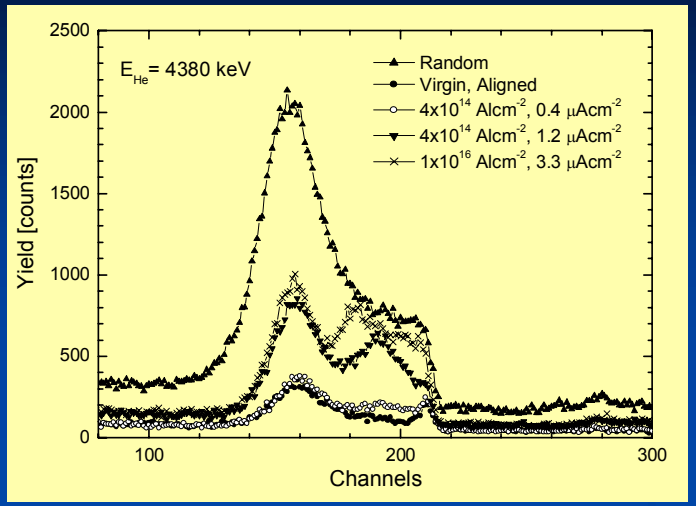

RBS spectra recorded on Al implanted 6H SiC

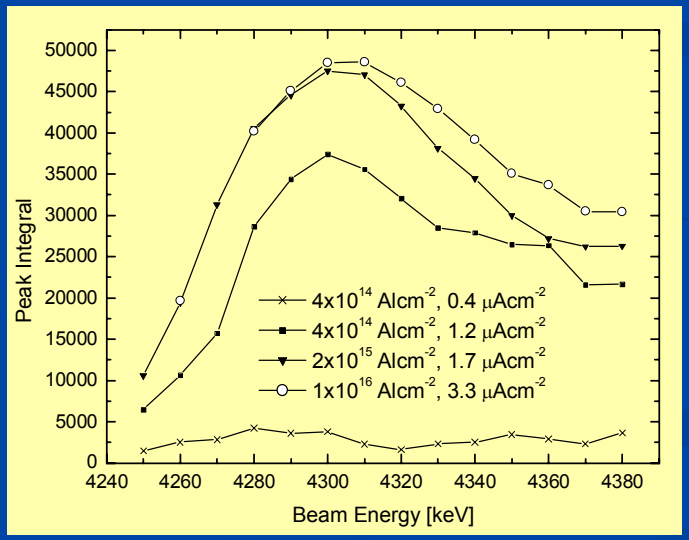

Deduced damage profile

Thank you for your attention!